nature communications

Article

https://doi.org/10.1038/s41467-025-55853-7

Autonomous ribosome biogenesis in vitro

Received: 19 June 2024

Accepted: 31 December 2024

Published online: 08 January 2025

Check for updates

Yuishin Kosaka[1,2], Yumi Miyawaki[1], Megumi Mori[1], Shunsuke Aburaya[3], Chisato Nishizawa[1], Takeshi Chujo[4,5], Tatsuya Niwa[6], Takumi Miyazaki[1], Takashi Sugita[7], Mao Fukuyama[5,8], Hideki Taguchi[6], Kazuhito Tomizawa[4], Kenji Sugase[1], Mitsuyoshi Ueda[1,9] & Wataru Aoki[5,9,10]

Ribosome biogenesis is pivotal in the self-replication of life. In *Escherichia coli*, three ribosomal RNAs and 54 ribosomal proteins are synthesized and subjected to cooperative hierarchical assembly facilitated by numerous accessory factors. Realizing ribosome biogenesis in vitro is a critical milestone for understanding the self-replication of life and creating artificial cells. Despite its importance, this goal has not yet been achieved owing to its complexity. In this study, we report the successful realization of ribosome biogenesis in vitro. Specifically, we developed a highly specific and sensitive reporter assay for the detection of nascent ribosomes. The reporter assay allowed for combinatorial and iterative exploration of reaction conditions for ribosome biogenesis, leading to the simultaneous, autonomous synthesis of both small and large subunits of ribosomes in vitro through transcription, translation, processing, and assembly in a single reaction space. Our achievement represents a crucial advancement toward revealing the fundamental principles underlying the self-replication of life and creating artificial cells.

The development of self-replicating artificial cells, or a self-replicating central dogma, has been a long-standing goal in synthetic biology, with the potential to drive profound scientific advances[1,2]. Building artificial cells requires attaining a deep understanding of cellular components and their organization, which would greatly enhance our comprehension of this complex, dynamic system. Furthermore, the ability to build artificial cells would enable scientists to create novel cell types beyond those found in nature, allowing them to explore the vast possibilities of life beyond its current form.

Ribosome biogenesis is pivotal in the self-replication of life, and it is universally conserved across living organisms. In *Escherichia coli*, three rRNAs (16S, 23S, and 5S) are transcribed by RNA polymerase, and 54 ribosomal proteins (r-proteins) are recursively synthesized by preexisting ribosomes as structural components[3,4]. They are cotranscriptionally assembled in a cooperative hierarchy through multiple parallel assembly pathways[5–14]. The assembly process is supported, modified, and modulated by numerous accessory factors[3,4]. All these steps concurrently occur in the cytoplasmic space in a highly coordinated manner, resulting in the synthesis of the 2.5-MDa 70S ribosome, consisting of the 30S small and 50S large subunits (SSU and LSU, respectively), in a few minutes[15]. The SSU and LSU, containing decoding and peptidyl transferase centers, respectively, are essential for translation. Ribosomes play multifaceted roles in healthy cells, and ribosome biogenesis dysregulation leads to the development of various aberrant states such as cell death and cancer[16]. The comprehensive understanding of ribosomes has enabled the design of artificial ribosomes with altered or enhanced functionalities[17–22].

Achieving ribosome biogenesis outside living cells is an essential step toward creating artificial cells, as synthesizing ribosomes from DNA is vital for building artificial cells. Intensive scientific efforts have been invested in to achieve ribosome assembly in vitro for decades. Ribosome assembly mapping revealed assembly order and

[1]Division of Applied Life Sciences, Graduate School of Agriculture, Kyoto University, Kyoto, Japan. [2]Japan Society for the Promotion of Science, Kyoto, Japan. [3]Division of Metabolomics, Medical Institute of Bioregulation, Kyushu University, Fukuoka, Japan. [4]Department of Molecular Physiology, Faculty of Life Sciences, Kumamoto University, Kumamoto, Japan. [5]JST FOREST, Tokyo, Japan. [6]Cell Biology Center, Institute of Integrated Research, Institute of Science Tokyo, Yokohama, Japan. [7]TechnoPro, Inc. TechnoPro R&D, Company, Tokyo, Japan. [8]Institute of Multidisciplinary Research for Advanced Materials, Tohoku University, Sendai, Japan. [9]Kyoto Integrated Science & Technology Bio-Analysis Center, Kyoto, Japan. [10]Department of Biotechnology, Graduate School of Engineering, Osaka University, Osaka, Japan. e-mail: aoki.wataru@bio.eng.osaka-u.ac.jp

intermediates, as well as thermodynamic and kinetic parameters[23–27]. The in vitro integrated synthesis, assembly, and translation (iSAT) realized the coupling of rRNA synthesis and ribosome assembly using purified r-proteins[28–31]. These methods have been widely used to provide critical insights into the mechanisms of ribosome assembly[5–8,10,11,32–35]. The efforts in nonautonomous ribosome assembly with purified r-proteins encouraged attempts to achieve ribosome biogenesis in vitro. One study aimed to cogenerate r-proteins from DNA templates in an in vitro one-pot reaction[36]. Another study conducted simultaneous expression of SSU structural components and specific accessory factors on a chip in an attempt to realize SSU biogenesis in vitro[37]. The latter reproduced several hallmarks of SSU biogenesis on a chip; however, nascent SSU activity as the decoding center was not confirmed[37]. To the best of our knowledge, there has never been an attempt at realizing in vitro LSU biogenesis, which is a far more complex process compared to SSU biogenesis[4]. Hence, a big leap needs to be made forward to realize ribosome biogenesis in vitro.

In this study, we report the successful ribosome biogenesis in vitro. We hypothesized that optimizing ribosomal component expression patterns in a cytoplasm-like reaction solution would yield in vitro ribosome biogenesis. Specifically, our approach involved coactivating the transcription of an operon encoding three rRNAs, the transcription and translation of 54 genes encoding r-proteins, and the assembly of ribosomes in an optimized *E. coli* S150 cell extract. Specifically, the optimized *E. coli* S150 cell extract contains the soluble *E. coli* proteome, including dozens of accessory factors for ribosome biogenesis[3,4], physiological ions abundant in the cytoplasm (magnesium glutamate and potassium glutamate)[28,38], polyamines important for transcription and translation (spermidine and putrescine)[39], and a reducing agent (DTT). To test our hypothesis, we developed a highly specific and sensitive reporter assay to detect the translational activity of nascent ribosomes by combining an orthogonal translation system[40–43] and a femtoliter droplet assay[44]. The reporter assay enabled combinatorial and iterative exploration of reaction conditions, leading to the simultaneous, autonomous synthesis of both SSU and LSU in vitro through transcription, translation, processing, and assembly in a single reaction space. Finally, we demonstrated that ribosomes composed of nascent artificial SSU and LSU were functional. Ribosome biogenesis in vitro allows more freedom in controlling the process of ribosome biogenesis. Therefore, this achievement could facilitate elucidating the ribosome assembly process[3,4], revealing fundamental principles underlying the self-replication of life, and creating self-replicating artificial cells[45].

Results and discussion

Development of a highly specific reporter assay for nascent ribosome detection

In an attempt to realize ribosome biogenesis in vitro, a highly specific and sensitive reporter assay for detection of the nascent ribosome translational activity would be required as preexisting and nascent ribosomes would coexist in a single reaction space. Translation initiation is mainly influenced by the RNA–RNA base pairing between the Shine–Dalgarno (SD) and anti-Shine–Dalgarno (ASD) sequences of mRNA and the 16S rRNA, respectively[46]. Consequently, the generation of new SD and ASD leads to the development of orthogonal translation systems[40–43] useful for detecting nascent artificial ribosomes (Fig. 1A). Among them, a two-sided orthogonal translation system would offer superior specificity and sensitivity. A previous study described that certain pairs of orthogonal SDs and ASDs (oSDs and oASDs, respectively) exhibit two-sided orthogonality in *E. coli*[41]. However, whether any oSD·oASD pairs exhibit two-sided orthogonality in vitro remains elusive[30].

We selected seven oSD·oASD pairs[41–43] (named a, b, c, d, or1, or4, and j) as candidates to screen two-sided orthogonal translation systems available in *E. coli* cell extracts (Supplementary Data 1). First, we designed an experimental scheme to select oSDs that do not interact with native ribosomes in the cell extracts (Fig. 1B). Using oSD–sfGFP reporters, we observed that six oSDs (b, c, d, or1, or4, and j) did not show any functional interaction with the native ribosomes (Fig. 1C). Two types of cell extracts (sonicated S12 or French press S30) showed similar profiles; hence, we used the S12 extracts for the following screening processes due to their ease of preparation. We thus further investigated the orthogonality of the four oSDs (b, or1, or4, and j), which were selected by an arbitrary selection criterion based on the mean fluorescence values in ascending order. We used LacZ reporters that were more sensitive than the GFP reporters, and discovered that three oSDs (b, or1, and or4) displayed orthogonality against the native ribosomes (Fig. 1D).

Next, we designed an experimental scheme to screen oSD·oASD pairs with two-sided orthogonality in cell extracts (Fig. 1E). We prepared functional cell extracts using *E. coli* expressing an artificial rRNA operon with WT-ASD or oASD (b, or1, or or4) and C1192U spectinomycin resistance (SpcR)[47] in the 16S rRNA (Supplementary Fig. 1A). The cell extracts containing artificial ribosomes with b-, or1-, or or4-oASD did not generate reporter signals when mixed with a WT-SD–LacZ reporter and spectinomycin (Fig. 1F and Supplementary Fig. 1B). When mixed with the cognate oSD–LacZ reporter and spectinomycin, the cell extracts containing artificial ribosomes with b-, or1-, and or4-oASD generated reporter signals (Fig. 1G). Based on these results, we selected the or1-oSD·oASD pair as the two-sided orthogonal translation system. We verified in a follow-up control experiment that the reporter signals originated from the or1-oSD·oASD pairing, not from SpcR (Supplementary Fig. 1C). In addition, the or1-orthogonal translation system exhibited a higher residual reporter signal than the native translation system in the presence of mRNAs with WT-SD (Supplementary Fig. 1D), as it only translates the reporter mRNA with the cognate or1-SD. This characteristic is valuable in an attempt to realize ribosome biogenesis in vitro, where mRNAs encoding r-proteins and a reporter mRNA for nascent ribosome detection coexist in the same reaction space.

Encouraged by the success to develop the highly specific reporter assay, we conducted a preliminary trial to realize SSU biogenesis in vitro. However, we observed no nascent SSU-derived reporter signal (Supplementary Fig. 2), confirming the difficulty in activating such a complex process in vitro. Under nonoptimized reaction conditions, if nascent artificial SSU was synthesized, its amount is expected to be insufficient for detection by fluorescence microplate readers. Thus, we deduced that a more sensitive assay would be required to allow the combinatorial and iterative exploration of reaction conditions that would enable ribosome biogenesis in vitro.

Highly sensitive detection of the artificial ribosome translational activity

We devised an automated femtoliter droplet assay for sensitive, scalable, and objective detection of artificial ribosome translational activity. In a femtoliter droplet assay, an enzyme-containing reaction solution is confined to femtoliter droplets, increasing the effective concentration of the enzyme and inhibiting the diffusion of the reaction products. Even when the concentration of the enzyme in the reaction solution is extremely low, confinement to femtoliter droplets ensures the highly sensitive detection of enzymatic activity (Fig. 2A)[44]. We developed a deep-learning-assisted automated analysis pipeline for a droplet assay (Supplementary Fig. 3) using a trained U-Net deep-learning model[48,49]. The analysis pipeline allows the automated binary segmentation of images (droplet or background) and extraction of features of each droplet (size and fluorescence intensity), enabling scalable and objective analysis of droplet assays.

Next, we evaluated the sensitivity of the droplet assay. We prepared two types of S12 cell extracts: one contained native ribosomes and 1.2 μM of artificial ribosomes with or1-oASD and SpcR (refer to Quantification of the artificial ribosome

https://doi.org/10.1038/s41467-025-55853-7

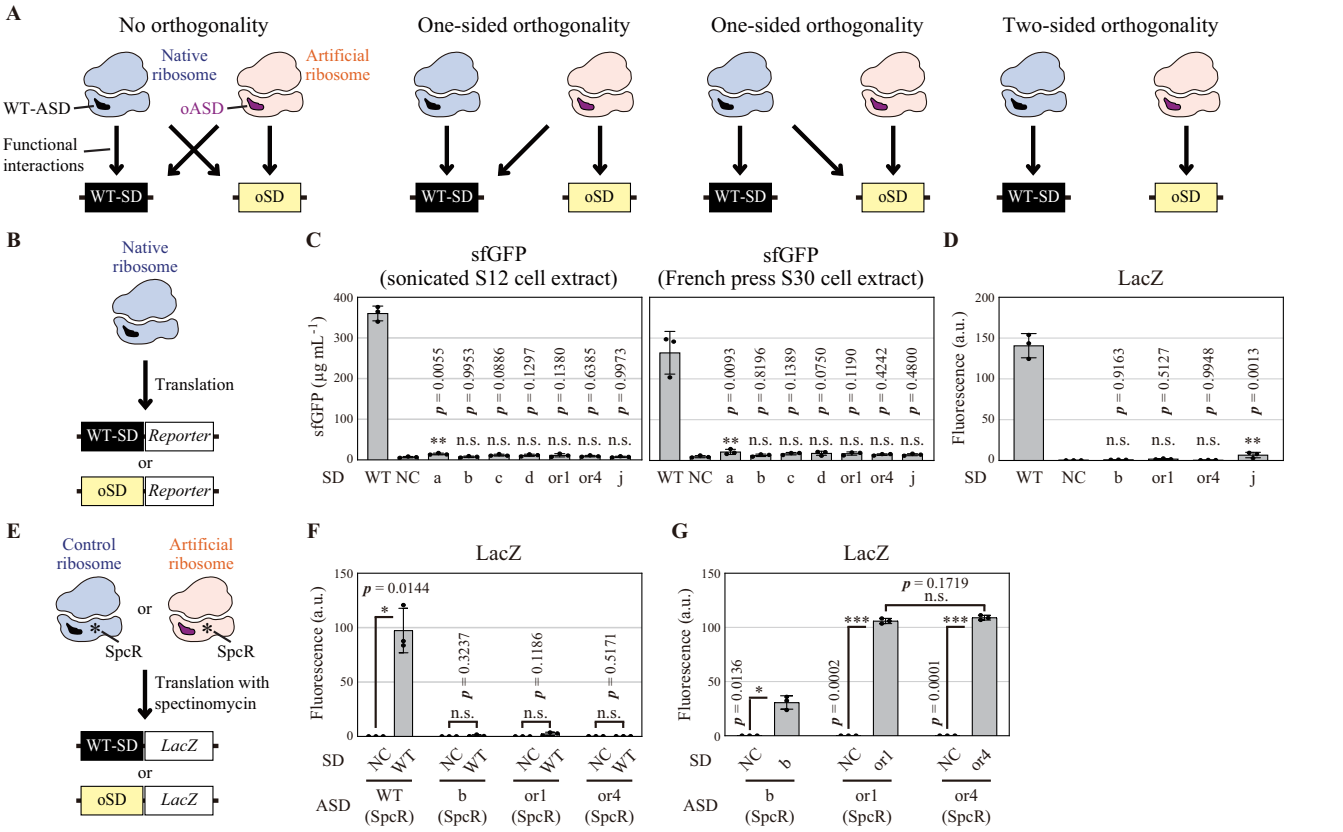

Fig. 1 | Screening orthogonal oSD·oASD pairs with two-sided orthogonality in vitro. A Four types of orthogonalities. SD, Shine–Dalgarno sequence; ASD, anti-Shine–Dalgarno sequence; oSD, orthogonal SD; oASD, orthogonal ASD. **B** Experimental scheme to screen oSDs that do not interact with native ribosomes in cell extracts. Fluorescence was detected using fluorescence microplate readers. **C** oSD selection. Either a WT-SD–sfGFP or an oSD–sfGFP reporter (named a, b, c, d, or1, or4, and j) was mixed with S12 or S30 cell extracts. NC, negative control without a reporter. Mean ± SD ($n = 3$). **, $p < 0.01$; n.s., not significant; one-way ANOVA with Dunnett's test against NC. **D** Further oSD selection. Either a WT-SD–LacZ or an oSD–LacZ reporter (b, or1, or4, and j) was mixed with S12 cell extracts. a.u., arbitrary unit. Mean ± SD ($n = 3$). One-way ANOVA with Dunnett's test against NC. **E** Experimental scheme to screen oSD·oASD pairs with two-sided orthogonality in cell extracts. Cell extracts were prepared using BL21 Star™ (DE3) *lacZ::frt* expressing an artificial rRNA operon with WT-ASD or oASD (b, or1, or or4) and C1192U spectinomycin resistance (SpcR). **F** Screening oASDs that do not interact with the WT-SD–LacZ reporter. The cell extracts were mixed with the WT-SD–LacZ reporter and spectinomycin. Mean ± SD ($n = 3$). *, $p < 0.05$; two-tailed Welch's *t*-test. **G** Screening oSD·oASD pairs with two-sided orthogonality. The cell extract was mixed with the cognate oSD–LacZ reporter and spectinomycin. Mean ± SD ($n = 3$). ***, $p < 0.001$; two-tailed Welch's *t*-test. Three biological replicates were used in all experiments. Source data are provided as a Source Data file.

concentration in S12 cell extract in Materials and Methods), and the other was a control cell extract containing only native ribosomes. We performed a control experiment by mixing the control cell extract with the or1-oSD–LacZ reporter. Unexpectedly, we observed native ribosome-derived fluorescence in the droplet assay (Supplementary Fig. 4A), which was not detected in the bulk assay (Fig. 1D), indicating the high sensitivity of the droplet assay. We observed that the combined use of the orthogonal reporter with spectinomycin enabled us to specifically detect the artificial ribosome translational activity (Supplementary Fig. 4). Then, to evaluate the sensitivity of the assay, we diluted the cell extract containing the artificial ribosomes using the control cell extract and mixed it with the or1-oSD–LacZ reporter and spectinomycin. As a result, we successfully detected the translational activity of the artificial ribosomes even at 12 pM (10^5 dilution ratio) (Fig. 2B). Our Poisson distribution-based calculation, assuming that the artificial ribosomes in the cell extract did not form polysomes, suggested that the assay enabled translational activity detection down to the single-ribosome level (Supplementary Fig. 5). We found that small droplets exhibited increased translational activity. Although the underlying mechanism remains unclear, the ratio of surface area to volume may influence gene expression, as previously reported[50,51].

SSU biogenesis in vitro

We revisited SSU biogenesis in vitro using the two-sided orthogonal translation system and the droplet assay. We hypothesized that combinatorial optimization of the ribosomal component expression patterns in a cytoplasm-like reaction solution would result in in vitro ribosome biogenesis. Our experimental scheme was divided into two sequential reactions (Fig. 3A). In the first reaction, we aimed at coactivating the transcription of the artificial rRNA operon with or1-oASD and SpcR, the transcription and translation of 21 SSU r-protein genes, and the assembly in the optimized *E. coli* S150 cell extract. The second reaction was designed for detecting nascent artificial SSU translational activity using the or1-oSD–LacZ reporter. We observed no reporter signal during the initial trial attempting SSU biogenesis in vitro, even using the droplet assay, confirming again the difficulty in realizing SSU biogenesis in vitro (Supplementary Fig. 6A). Then, we thoroughly explored the reaction conditions using a simplex-lattice design and optimized the concentrations of the native ribosomes, the artificial rRNA operon, and 21 SSU r-protein genes. We hypothesized that increasing ribosomal gene concentrations could be beneficial to activating SSU biogenesis as higher DNA concentrations usually produce robust expression profiles[52]. However, contrary to our expectations, reducing their concentrations was pivotal and led to slight reporter signal detection using the droplet assay (Fig. 3B). We conducted a

https://doi.org/10.1038/s41467-025-55853-7

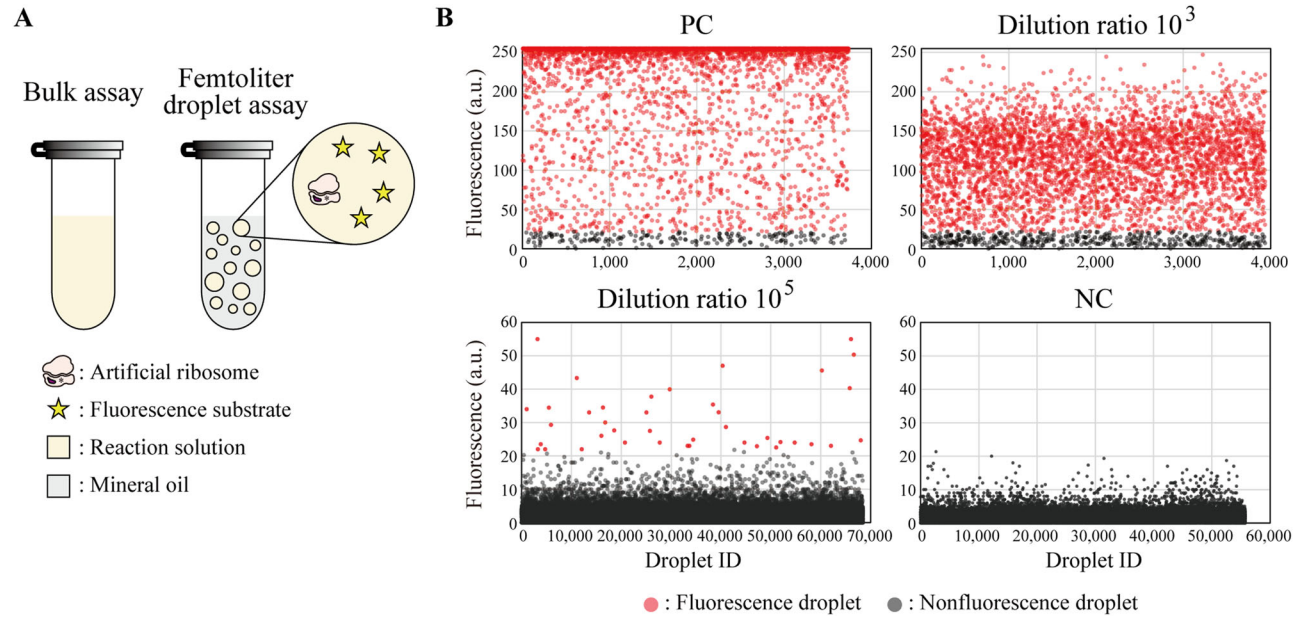

Fig. 2 | Highly sensitive detection of the artificial ribosome translational activity. A Comparison between a conventional bulk assay and a femtoliter droplet assay. **B** Detection of the translational activity of the artificial ribosomes using the droplet assay. We prepared two types of S12 cell extracts; one contained native ribosomes and 1.2 μM of artificial ribosomes with or1-oASD and C1192U spectinomycin resistance (SpcR) and the other only native ribosomes. The cell extract containing the artificial ribosomes was diluted by the control cell extract at the indicated ratio. The cell-free transcription and translation in droplets were carried out in the presence of the or1-oSD–LacZ reporter and spectinomycin. In the scatter plots, the vertical and horizontal axes indicate the mean fluorescence intensity and the ID of each droplet, respectively. Droplets exceeding the threshold (mean fluorescence intensity ≥ 22) are indicated in red. The threshold was set at a value that none of the droplets in the negative control exceeded. PC, positive control without dilution; NC, negative control using only the control cell extract; a.u., arbitrary unit. Source data are provided as a Source Data file.

follow-up optimization and successfully optimized the reaction conditions that generated almost saturated reporter signals in the droplet assay (Fig. 3C and Supplementary Fig. 6B). Using the optimized reaction condition, we detected a strong, nascent artificial SSU-derived fluorescence signal even in the bulk assay (Fig. 3D). Based on the calibration curve, we determined that the in vitro SSU biogenesis produced a signal corresponding to 9.8 nM ribosomes (Supplementary Fig. 6C). In comparison to the autonomous assembly, we also determined that the iSAT reaction produced a signal corresponding to 2.8 nM ribosomes (Supplementary Fig. 6D). The autonomous assembly reported here and the nonautonomous iSAT assembly are different processes with different optimal conditions[53]. Future studies are expected to clarify the difference between these processes by examining the specific effects of each optimal reaction condition.

Although the underlying mechanism explaining the critical role of reduced DNA concentrations remains unclear, two main possibilities could explain this observation. The first possibility involves energy depletion in cell-free transcription and translation (CF-TXTL) systems. Excessive transcription may consume a substantial amount of energy, leaving insufficient energy for translation. The second possibility is that high mRNA concentrations could inhibit translation owing to an imbalance between mRNA and various translation components, such as formyl-Met-tRNA and initiation factors, potentially leading to the formation of inactive translation complexes[54].

LSU biogenesis in vitro

We moved ahead to realize LSU biogenesis in vitro. Our experimental scheme was similar to that for SSU (Fig. 4A). The first reaction consisted of coactivating the transcription of an artificial rRNA operon with A2058U clindamycin resistance (CldR)[55] in the 23S rRNA, the transcription and translation of 33 LSU r-protein genes, and the assembly in the optimized S150 cell extract. The second reaction was designed for detecting nascent artificial LSU translational activity using the WT-SD–LacZ reporter in the presence of 1.5 mM clindamycin, a concentration sufficient to inhibit the native ribosomes (Supplementary Fig. 7A). We expected that detection of the nascent artificial LSU translational activity would be difficult for three reasons: i) LSU biogenesis is far more complex than SSU biogenesis[4], ii) the two-sided orthogonal translation system is not available as the nascent artificial LSU requires native SSU for translation, and iii) ribosomes with the A2058U ClдR mutation retain only ~42% of their translational activity in the presence of 1.5 mM clindamycin (Supplementary Fig. 7B). Surprisingly, a simple exploratory experiment in the bulk assay based on the optimized reaction condition for SSU biogenesis in vitro enabled us to detect significant fluorescence signals derived from the nascent artificial LSU (Fig. 4B, C). As expected, the fluorescence signal obtained from the nascent artificial LSU was lower than that from the nascent artificial SSU (Figs. 3D and 4C). To enhance the fluorescence signal, we constructed an improved LacZ reporter regulated by the *pT7CONS*[56] and *EpsA20*[57] 5′UTR sequences to improve transcription and translation efficiency. Using the improved LacZ reporter, we successfully enhanced by 3.8-fold the nascent artificial LSU-derived fluorescence signal (Fig. 4D). Based on the calibration curve, we determined that the in vitro LSU biogenesis produced a signal corresponding to 3 nM ribosomes (Supplementary Fig. 7C).

We tried to characterize the properties of our reaction systems. First, we investigated r-protein production profiles using heavy L-arginine ($^{13}C_6$, $^{15}N_4$) and L-lysine ($^{13}C_6$, $^{15}N_2$) to label nascent r-proteins during SSU and LSU biogenesis in vitro. Our mass spectrometric analyzes revealed that nascent r-proteins originated from the plasmids encoding r-proteins but not from residual *E. coli* chromosomal fragments or mRNAs in the S150 cell extracts (Supplementary Fig. 8A). The mass spectrometric analyzes were unable to identify bL35 and bL36, as these small, basic proteins are challenging targets for mass spectrometry[36]. Two main reasons explain this difficulty. First, during pretreatment for mass spectrometry, proteins are purified by precipitation, and small proteins tend to exhibit low precipitation efficiency. Second, mass spectrometry typically relies on identifying peptides produced through

https://doi.org/10.1038/s41467-025-55853-7

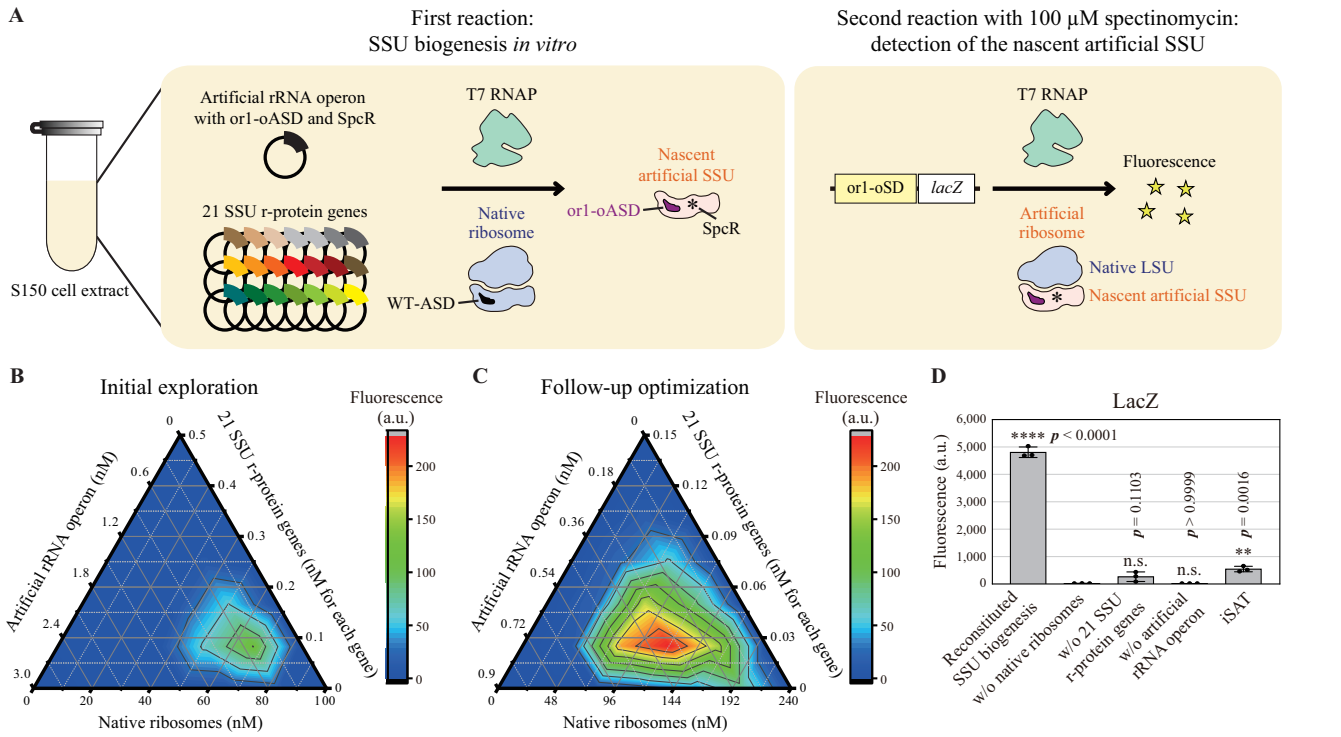

Fig. 3 | SSU biogenesis in vitro. A Experimental scheme for SSU biogenesis in vitro. **B** Exploring optimal conditions for the first reaction using a simplex-lattice design. In the first reaction, the concentrations of the native ribosomes, the artificial rRNA operon with or1-oASD and C1192U spectinomycin resistance (SpcR), and 21 SSU r-protein genes were 0–100, 0–3, and 0–0.5 nM each, respectively. The second reaction was conducted with the or1-oSD–LacZ reporter and spectinomycin using the droplet assay. The data represent the mean fluorescence intensity of droplets. a.u., arbitrary unit. **C** Follow-up optimization of the first reaction. In the first reaction, the concentrations of the native ribosomes, the artificial rRNA operon, and 21 SSU r-protein genes were 0–240, 0–0.9, and 0–0.15 nM each, respectively. The second reaction was conducted with the or1-oSD–LacZ reporter and spectinomycin using the droplet assay. The optimal reaction condition was a native ribosome concentration of 120 nM. However, in the following experiments, we selected suboptimal reaction conditions with 80 nM native ribosomes to reduce reagent costs. **D** Successful detection of the nascent artificial SSU translational activity using the bulk assay under the optimized reaction condition. In the first reaction, the concentrations of the native ribosomes, the artificial rRNA operon, and 21 SSU r-protein genes were 80, 0.3, and 0.05 nM each, respectively. The second reaction was conducted with the or1-oSD–LacZ reporter and spectinomycin using the bulk assay. Mean ± SD ($n = 3$, biological replicates). ****, $p < 0.0001$; **, $p < 0.01$; n.s., not significant; one-way ANOVA with Dunnett's test against the negative control without native ribosomes. The p-values showing $p < 0.0001$ and $p > 0.9999$ are $p = 1.0 \times 10^{-5}$ and $p = 9.9999 \times 10^{-1}$, respectively. Source data are provided as a Source Data file.

trypsin digestion; however, small, basic proteins are less likely to contain peptides with high ionization efficiency. To overcome these challenges, we used lysine-charged tRNA labeled with the fluorophore BODIPY to specifically label nascent proteins, confirming that bL35 and bL36 were efficiently expressed in the S150 extract (Supplementary Fig. 8B). Second, we tried to obtain direct evidence for the incorporation of newly synthesized r-proteins into nascent ribosomes. We conducted an experiment using a mutant r-protein gene encoding uS12 K43T, which confers streptomycin resistance (StrR) to ribosomes[58]. uS12 K43T was reportedly used for assessing nascent r-protein incorporation[30]. We observed that the reporter signals remained unaffected by streptomycin only when we used the mutant r-protein gene as the starting material, indicating the successful autonomous assembly of ribosomes consisting of uS12 K43T (Supplementary Fig. 8C). Third, we investigated whether adding extra LSU or SSU improves the in vitro SSU and LSU biogenesis by alleviating the imbalanced stoichiometries. We observed no significant differences in fluorescence signals in either the in vitro SSU or LSU biogenesis with extra LSU or SSU, respectively (Supplementary Fig. 8D). This is probably because the imbalanced stoichiometries of the nascent SSU and LSU were not extremely large. Fourth, we confirmed whether physiological salts in the optimized S150 cell extract are required for the in vitro SSU and LSU biogenesis. We performed SSU and LSU biogenesis in vitro using the S150 cell extracts dialyzed with physiological salts (potassium and glutamate), as used throughout this study, and S150 cell extracts dialyzed with non-physiological salts (ammonium and chloride)[28]. The biogenesis of SSU and LSU consequently occurred only in the cell extracts dialyzed with physiological salts (Supplementary Fig. 8E). Fifth, we investigated whether nascent rRNAs and r-proteins exhibited modifications observed in native ribosomes. To purify nascent rRNAs, we used nascent artificial 16S and 23S rRNAs with streptavidin-binding aptamer (Sb-aptamer)[59,60] in the in vitro SSU and LSU biogenesis. The resultant nascent artificial SSU and LSU with Sb-aptamer were purified using streptavidin resin under a subunit dissociation condition (1 mM Mg^{2+}), enabling the successful isolation of nascent artificial SSU and LSU with high purity (Supplementary Fig. 9). Mass spectrometry identified modifications such as $m^6{}_2A$, m^1G, Gm, m^6A, Cm, m^5C, Ψ, m^2G, and m^7G in the nascent artificial rRNAs and native *E. coli* rRNAs (Supplementary Fig. 10). m^2A and m^5U were almost absent in the nascent artificial rRNAs (Supplementary Fig. 10). The near absence of m^2A and m^5U could be attributable to the responsible non-essential enzymes (RlmN, RlmC, and RlmD) containing the iron-sulfur cluster[61,62], which is susceptible to oxygen. Furthermore, we analyzed nascent r-proteins labeled with heavy amino acids via mass spectrometry and identified some post-translational modifications such as N-terminal methionine excision of uS8, uS9, and uS12 and glutamine methylation of uL3 (Supplementary Fig. 11).

Nascent artificial ribosomes are functional

We investigated whether SSU and LSU biogenesis could be simultaneously activated in a single reaction space. We coactivated the transcription of an artificial rRNA operon with or1-oASD, SpcR in the 16S rRNA, and CldR in the 23S rRNA, and the production of 54 r-proteins in

https://doi.org/10.1038/s41467-025-55853-7

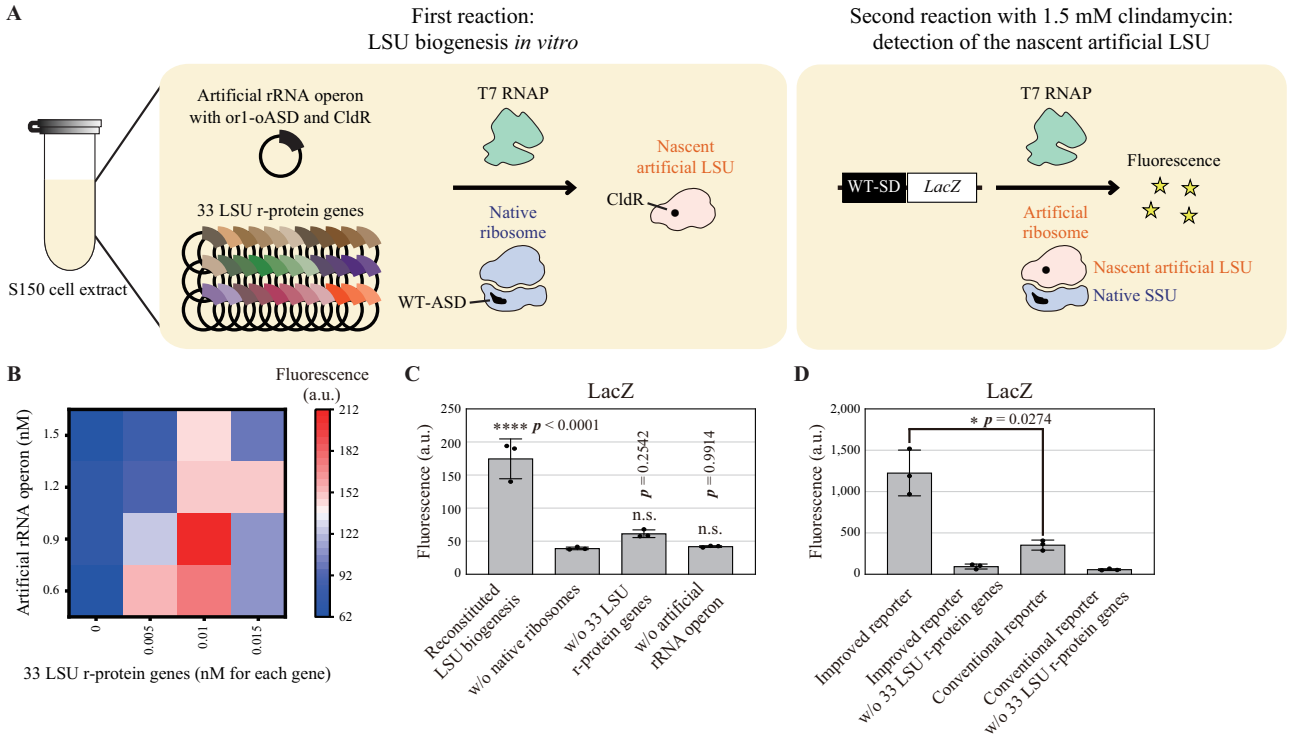

Fig. 4 | LSU biogenesis in vitro. A Experimental scheme for LSU biogenesis in vitro. **B** Exploring optimal conditions for the first reaction. In the first reaction, the concentrations of the native ribosomes, artificial rRNA operon with A2058U clindamycin resistance (CldR), and 33 LSU r-protein genes were 80, 0.6–1.5, and 0–0.015 nM each, respectively. The second reaction was conducted with the WT-SD–LacZ reporter and clindamycin using the bulk assay. a.u., arbitrary unit. **C** Reproducible detection of the nascent artificial LSU translational activity under the optimized reaction condition. In the first reaction, the concentrations of the native ribosomes, the artificial rRNA operon, and 33 LSU r-protein genes were 80, 0.9, and 0.01 nM each, respectively. The second reaction was conducted with the WT-SD–LacZ reporter and clindamycin using the bulk assay. Mean ± SD ($n = 3$, biological replicates). ****, $p < 0.0001$; n.s., not significant; one-way ANOVA with Dunnett's test against the negative control without native ribosomes. The p-value showing $p < 0.0001$ is $p = 1.0 \times 10^{-5}$. **D** Improvement of the nascent LSU-derived fluorescence signal. The experimental condition was the same as Fig. 4C except that an improved LacZ reporter with a modified 5′UTR sequence was used instead of the WT-SD–LacZ reporter. The signal-to-noise ratio was improved because the background translation by the native ribosomes was sufficiently suppressed by 1.5 mM clindamycin (Supplementary Fig. 7A). Mean ± SD ($n = 3$, biological replicates). *, $p < 0.05$; two-tailed Welch's t-test. Although the experimental conditions in lane 1 in Fig. 4C and lane 3 in Fig. 4D were identical, they showed different values because these experiments were performed on different days. Source data are provided as a Source Data file.

the optimized reaction condition for the in vitro LSU biogenesis (Fig. 5A), leading to the successful synthesis of both LSU and SSU in a single reaction space (Fig. 5B). Surprisingly, the simultaneous synthesis of nascent artificial SSU and LSU was achieved in the same reaction condition for the in vitro LSU biogenesis. This is probably because the most challenging part of ribosome biogenesis is LSU biogenesis[4], and in an environment in which LSU biogenesis is possible, the simultaneous synthesis of SSU and LSU was likely possible if the available resource was sufficient. As expected, we did not observe a significant signal under the double-antibiotic condition (Fig. 5B). This is because SSU and LSU are freely interchangeable. In each translation cycle, native and artificial subunits in the pool randomly associate at translation initiation. Under the single-antibiotic conditions, nascent artificial SSU or LSU can initiate dozens of translation cycles. Under the double-antibiotic condition, however, nascent artificial subunits were deactivated before a sufficient amount of reporter proteins was produced. Even in vivo, in which large amounts of artificial SSU and LSU can be produced, detecting the translational activity of artificial ribosomes composed of artificial SSU and LSU in the presence of native subunits is challenging[18,19]. Detecting nascent artificial ribosome translational activity is assumed to be challenging, even with the droplet assay. If we assume that SSU and LSU interact randomly and that several nM of nascent artificial SSU and LSU are produced in the presence of 80 nM native ribosomes, the estimated concentration of nascent artificial ribosomes would be less than single-digit pM, which is below the droplet assay's detection limit (Fig. 2B). To investigate whether artificial ribosomes consisting of nascent artificial SSU and LSU are functional, we separately produced nascent artificial SSU and LSU with Sb-aptamer by the in vitro SSU and LSU biogenesis, respectively. These subunits were purified using streptavidin resin under the subunit dissociation condition (1 mM Mg^{2+}), as described in Supplementary Fig. 9C, removing native subunits. Although the yield of purification using Sb-aptamer and streptavidin resin was not high (~10%)[60], we successfully detected translational activity under the double-antibiotic condition only when we mixed the purified nascent artificial SSU and LSU, indicating that artificial ribosomes composed of these subunits were functional (Fig. 5C). Finally, we analyzed the protein composition of the artificial ribosomes assembled from the purified nascent artificial SSU and LSU by mass spectrometry (Supplementary Fig. 12). The result indicated that the artificial ribosomes were mainly composed of nascent r-proteins. Some r-proteins (uS2, bS21, uL1, bL9, uL10, bL12, and bL33) comprised both nascent and native r-proteins. This observation was consistent with previous research indicating that these r-proteins were interchangeable between ribosomes[63–66]. The interchangeability of these r-proteins is a property of ribosomes, and the synthesis of fully nascent ribosomes might be difficult in the context in which *E. coli* ribosomes synthesize *E. coli* ribosomes. Recently, a study proposed the use of heterologous ribosomes consisting of rRNAs and r-proteins derived from phylogenetically distant microorganisms for ribosome engineering in *E. coli*[67]. Such a framework might be useful for synthesizing fully nascent ribosomes without r-protein interchangeability.

https://doi.org/10.1038/s41467-025-55853-7

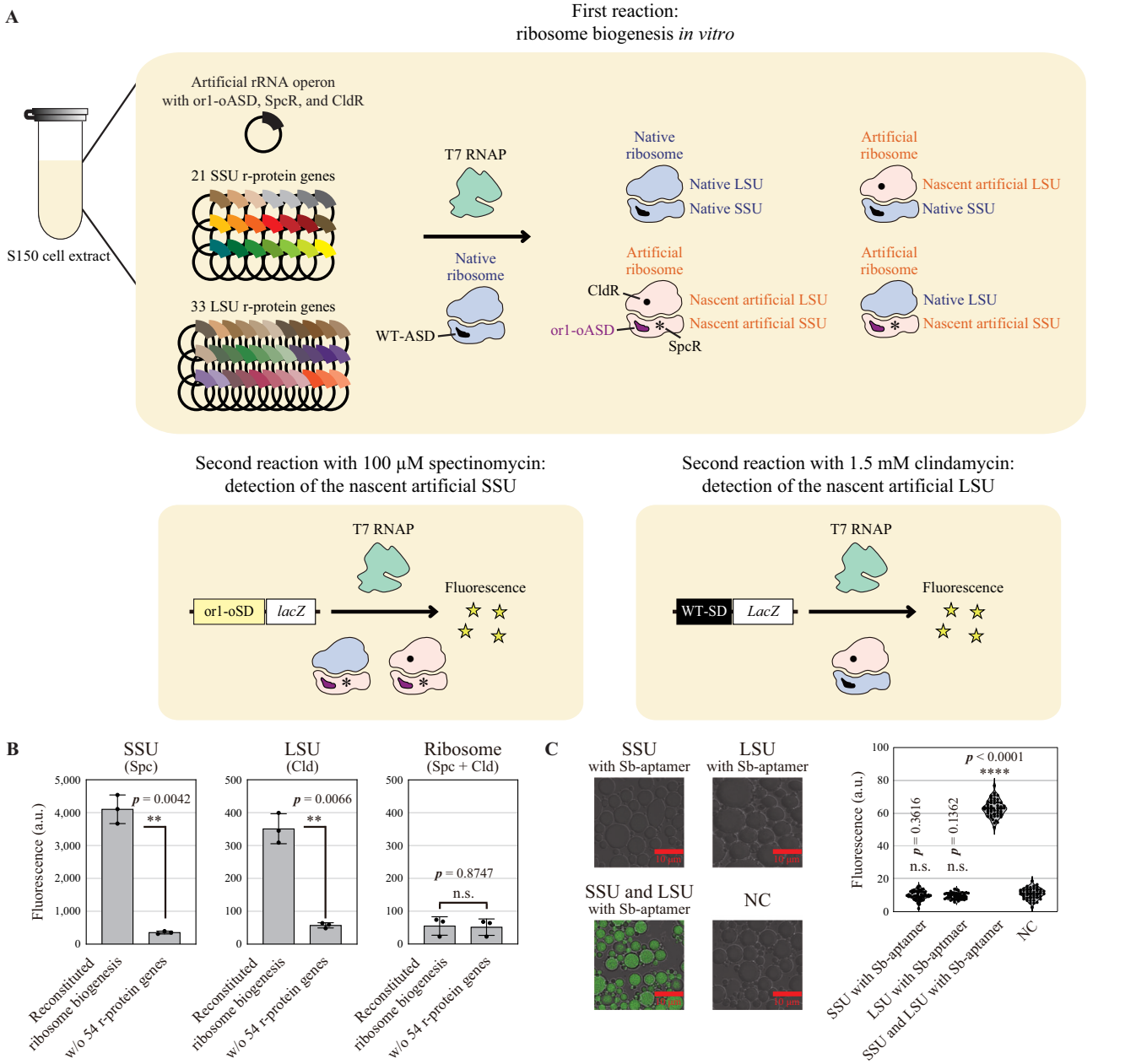

Fig. 5 | Synthesis of ribosomes in vitro. A Scheme showing in vitro synthesis of both SSU and LSU in a single reaction space. **B** Successful detection of the nascent artificial SSU and LSU translational activity in the bulk assay. In the first reaction, the concentrations of the native ribosomes, artificial rRNA operon with or1-oASD, C1192U spectinomycin resistance (SpcR), and A2058U clindamycin resistance (CldR), and 54 r-protein genes were 80, 0.9, and 0.01 nM each, respectively. The second reactions using the bulk assay were conducted with the or1-oSD–LacZ reporter and spectinomycin for the nascent artificial SSU, the improved LacZ reporter and clindamycin for the nascent artificial LSU, the or1-oSD–LacZ reporter, spectinomycin, and clindamycin for the nascent artificial ribosomes. a.u., arbitrary unit. Mean ± SD ($n = 3$, biological replicates). **, $p < 0.01$; n.s., not significant; two-tailed Welch's *t*-test. **C** Successful detection of the nascent artificial ribosome translational activity. The nascent artificial SSU (SpcR) and LSU (CldR) with streptavidin-binding aptamer (Sb-aptamer) were synthesized by the in vitro SSU and LSU biogenesis, respectively, and purified using streptavidin resin under the subunit dissociation condition (1 mM Mg^{2+}), as described in Supplementary Fig. 9C. We observed translational activity under the double-antibiotic condition only when we mixed the purified nascent artificial SSU and LSU. NC, negative control prepared using the same production and purification procedure without expressing the artificial rRNA operon with Sb-aptamer. Violin plot represents the mean fluorescence intensity values of droplets from three independent experiments. ****, $p < 0.0001$; one-way ANOVA with Dunnett's test against NC. Scale bars = 10 μm. The *p*-value showing $p < 0.0001$ is $p = 1.0 \times 10^{-5}$. Source data are provided as a Source Data file.

In this study, we realized ribosome biogenesis in vitro, solving a long-standing challenge in synthetic biology. This achievement provides greater ability to control the process of ribosome biogenesis, paving the way to reveal fundamental principles underlying ribosome biogenesis. Furthermore, our study brings the bottom-up creation of self-replicating artificial cells within reach as life scientists have successfully activated in vitro all of the major processes necessary for the autonomous central dogma, i.e., DNA replication[68,69], transcription[70], translation[71,72], and in this study, ribosome biogenesis. However, to achieve continuous self-replication, further improvements in ribosome biogenesis in vitro is required. In this study, 9.8 nM SSU and 3 nM LSU were synthesized from 80 nM native ribosomes, resulting in reproduction ratios of 12% (9.8/80 × 100) and 3.8% (3/80 × 100), respectively. Given that continuous self-replication requires each

ribosome to synthesize one or more ribosomes, a minimum 26-fold improvement is necessary. To fully realize this endeavor, improvements in CF-TXTL systems will be important. Although the protein synthesis capacity of current CF-TXTL systems lags behind that of living cells, these systems are continually being improved by ongoing research[73]. In the foreseeable future, the creation of self-replicating artificial cells in vitro may become a reality.

Methods

Strains and plasmids

The chromosomal *lacZ* gene of the BL21 Star™ (DE3) (Thermo Fisher Scientific, Waltham, MA, USA) was disrupted by Red-mediated recombination[74]. Briefly, pKD46 encoding phage λ-Red recombinase was transformed into the *E. coli* cells. The transformants were grown in 50 mL of SOC medium with 100 μg/mL ampicillin (Viccillin® for injection, Meiji Seika Pharma, Tokyo, Japan) and 10 mM L-(+)-arabinose (Nacalai Tesque, Kyoto, Japan). The fragment of the kanamycin-resistance gene (*kmr*) was amplified using primers (H1P1 forward primer, 5′-GAAATTGTGAGCGGATAACAATTTCACACAGGAAACAGCTGT GTAGGCTGGAGCTGCTTC-3′, and P4H2 reverse primer, 5′-TTACG CGAAATACGGGCAGACATGGCCTGCCCGGTTATTAATTCCGGGGATC CGTCGACC-3′) from pKD13, and introduced into the *E. coli* cells by electroporation. The electroporated cells were grown on an LB agar plate with 50 μg/mL of kanamycin monosulfate (Nacalai Tesque) to select Km^R transformants. The resulting strain is described as BL21 Star™ (DE3) *lacZ::kmr*. The FLP helper plasmid, pCP20, was transformed into the BL21 Star™ (DE3) *lacZ::kmr* to eliminate the *kmr* gene. As pCP20 harbors a temperature-sensitive replicon and shows thermal induction of FLP synthesis, the transformants were cultured non-selectively at 37 °C and tested for the loss of antibiotic resistance. The resulting strain is described as BL21 Star™ (DE3) *lacZ::frt*.

The steps to construct *E. coli* expressing an artificial rRNA operon with A2058U CldR instead of native rRNA operons were described below. We used *E. coli* SQ171/pCSacB/ptRNA100[75] (Addgene bacterial strain #155206) as the parental strain because this strain lacks chromosomal *rRNA* alleles and carries pCSacB as the source of the *rRNA* gene and a kanamycin resistance gene. *E. coli* SQ171/pCSacB/ptRNA100 was transformed with a plasmid encoding an artificial rRNA operon with A2058U CldR (pRRNA_CldR) and an ampicillin resistance gene. The transformant was grown in 5 mL of LB medium containing 100 μg/mL ampicillin, 100 μg/mL spectinomycin, and 0.25% sucrose to eliminate pCSacB. Loss of pCSacB was confirmed through the kanamycin sensitivity of the clones.

Plasmids were generated as follows. The *rrnB* rRNA operon was inserted into pET-41a(+) and regulated by the T7 promoter. Although T7 RNA polymerase (T7 RNAP) exhibits a higher transcription speed than that of *E. coli* RNA polymerase, which may result in different effects[76,77], we chose to use T7 RNAP in this study owing to its ease of use as a single-domain protein. Additionally, it has been reported that a T7 promoter-driven *rRNA* operon can successfully produce functional ribosomes[29,34]. Genes encoding 54 r-proteins were cloned from the *E. coli* DH5α genome. In this study, we included bS1 in r-proteins, which works more as a translational factor than a structural component, because additional bS1 could improve protein yields[78–81]. The expression of the genes encoding 54 r-proteins was regulated by the *pT7CONS*[56] and *EpsA20*[57] sequences, improving transcription and translation efficiencies. *pT7CONS* and *EpsA20* were also used to construct an improved LacZ reporter. Mutations in genes encoding rRNAs and r-proteins were introduced using mutagenic primer-based PCR.

The strains and plasmids used in this study are listed in Supplementary Data 2.

Sonicated S12 cell extract preparation

Sonicated S12 cell extracts were prepared as previously described with some modifications[82]. Specifically, *E. coli* cells were grown in 200 mL of 2 × YPTG medium at 37 °C. The cultured cells were harvested at OD_{600} of 3 and pelleted by centrifugation. The cell pellets were resuspended in 1 mL buffer A (10 mM Tris-HCl, 14 mM $Mg(OAc)_2$, 60 mM potassium glutamate, and 2 mM DTT, pH = 8.2) for 1 g of wet cell paste. The suspended cells were disrupted by a Q125 Sonicator (Qsonica, Newtown, CT, USA) at a frequency input of 20 kHz and amplitude of 50%. The sonication energy input was 500 J for 1 mL cell suspension. The cell extract was centrifuged at 4 °C and 12,000 *g* for 10 min, and the supernatant was collected. The obtained cell extract was flash-frozen in liquid nitrogen and preserved at −80 °C until further use.

French press cell extract preparation

French press S30 cell extracts were prepared based on previous reports with some modifications[28,29,83]. Briefly, *E. coli* cells were grown in 1 L of 2 × YPTG medium at 37 °C. The cultured cells were harvested at OD_{600} of 3 and pelleted by centrifugation. The cell pellets were resuspended in 4.5 mL buffer B (20 mM Tris-HCl, 100 mM NH_4Cl, 10 mM $MgCl_2$, 0.5 mM EDTA, and 2 mM DTT, pH = 7.2) for 1 g of wet cell paste. Halt Protease Inhibitor Cocktail (Thermo Fisher Scientific) and RNase Inhibitor (QIAGEN, Venlo, Netherlands) were added to the suspension. The cells were disrupted using an EmulsiFlex-C5 homogenizer (Avestin, Ottawa, Canada) with a single pass at a pressure of 20,000 psi. RNase Inhibitor and DTT were added to the cell extracts followed by centrifugation at 4 °C, 30,000 *g* for 30 min twice. The collected supernatant was dialyzed four times against the iSAT buffer (50 mM HEPES-KOH, 10 mM magnesium glutamate, 200 mM potassium glutamate, 2 mM DTT, 1 mM spermidine, and 1 mM putrescine)[83]. For clarification and concentration, the cell extract was centrifuged at 4000 *g* for 10 min in a Centriprep® 3 K device (EMD Millipore, Burlington, MA, USA). The obtained cell extract was flash-frozen in liquid nitrogen and preserved at −80 °C until further use.

French press S150 cell extracts were prepared as previously described with some modifications[28,29]. Specifically, BL21 Star™ (DE3) *lacZ::frt* harboring pT7_WT-ASD_rRNA was grown in 1 L of 2 × YPTG medium with 50 μg/mL of kanamycin at 37 °C until the OD_{600} reached 0.5. The cells were incubated with 0.1 mM isopropyl-β-D-thiogalactopyranoside (IPTG, Nacalai Tesque) and cultured until the OD_{600} reached 3. Then, the cells were disrupted using an EmulsiFlex-C5 homogenizer (Avestin) with a single pass at a pressure of 20,000 psi. The cell extracts were centrifuged at 30,000 *g* for 30 min at 4 °C. The collected supernatants were centrifuged at 90,000 *g* for 21 h at 4 °C. The collected supernatants were further centrifuged at 150,000 *g* for 3 h at 4 °C. In the centrifugation process, we omitted the sucrose cushion because we did not purify ribosomes in this process. Then, the collected supernatants were dialyzed using the iSAT buffer. The S150 extract with non-physiological salts was prepared by dialyzing the collected supernatants with buffer B. The cell extracts were concentrated using Amicon Ultra-15 3 kDa cutoff (Merck Millipore, Burlington, MA, USA). The obtained cell extract was flash-frozen in liquid nitrogen and preserved at −80 °C until further use.

Cell extract preparation containing ribosomes with artificial rRNAs

A plasmid encoding an artificial rRNA operon was introduced into the BL21 Star™ (DE3) *lacZ::frt*. The transformant was grown in a 2 × YPTG medium with 50 μg/mL of kanamycin at 37 °C until the OD_{600} reached 0.7. The cultured cells were incubated with 0.1 mM IPTG (Nacalai Tesque) for 3 h. The cell extracts were prepared as described above.

Cell-free transcription and translation (CF-TXTL)

CF-TXTL was performed according to a previous report with modifications[28]. *E. coli* ribosomes were purchased from New England BioLabs (Ipswich, MA, USA). T7 RNAP (New England BioLabs) was added to a final concentration of 0.8 U/μL. T7 RNAP was not added when we used cell extracts derived from IPTG-induced BL21 Star™

(DE3) or its derivative strains. The reporter plasmid concentration was 1.5 nM. The sfGFP or LacZ reporter expression was induced by IPTG at a final concentration of 2 mM. We used 5-chloromethylfluorescein di-β-D-galactopyranoside (CMFDG; Invitrogen, Waltham, MA, USA) as a substrate of LacZ at a final concentration of 33 μM. CF-TXTL was conducted using 15 μL reaction solutions at 37 °C in a 96-well plate (polystyrene, solid bottom, half area, black-walled, Greiner Bio-One International GmbH, Kremsmünster, Austria). The reporter signals were quantified using fluorescence microplate readers, Fluoroskan Ascent FL™ (Thermo Fisher Scientific) or Infinite® 200 PRO (TECAN, Männedorf, Switzerland), at λ_{ex} = 485 nm and λ_{em} = 535 nm. For native ribosome deactivation, spectinomycin (FUJIFILM Wako Pure Chemical Corporation, Osaka, Japan), streptomycin (FUJIFILM Wako Pure Chemical Corporation), or clindamycin (Abcam, Cambridge, UK) were used at final concentrations of 5 mM, 10 μg/mL, or 1.5 mM, respectively. The constituents of the CF-TXTL reaction solutions used in this study are summarized in Supplementary Data 3. For fluorescent labeling of nascent proteins, 1 μL of lysine-charged tRNA labeled with the fluorophore BODIPY (Promega Corporation, Madison, WI, USA) was added to the reaction solution.

SSU biogenesis in vitro was performed as follows. In the first reaction, 15 μL of the CF-TXTL solutions based on the S150 cell extracts were mixed with the native ribosomes, the artificial rRNA operon with or1-oASD and C1192U SpcR, and 21 SSU r-protein genes. We used S150 cell extracts to enable native ribosome concentration control. The solutions were incubated at 37 °C for 180 min. In the second reaction, the resulting CF-TXTL solutions were mixed with pT7_or1-oSD_LacZ, CMFDG, spectinomycin, and an additional 15 μL of the CF-TXTL solutions based on the S150 cell extracts. The fluorescence of the reaction solutions was measured using the bulk assay or the droplet assay. In the bulk assay, the reporter signals were kinetically measured at 37 °C using Infinite® 200 PRO (TECAN) at λ_{ex} = 485 nm and λ_{em} = 535 nm.

LSU biogenesis in vitro was performed as follows. In the first reaction, 15 μL of the CF-TXTL solutions based on the S150 cell extracts were mixed with the native ribosomes, the artificial rRNA operon with or1-oASD, SpcR, and A2058U CldR, and 33 LSU r-protein genes. The solutions were incubated at 37 °C for 180 min. In the second reaction, the resulting CF-TXTL solutions were mixed with pT7_WT-SD_LacZ or pT7PCONS_EpsA20_WT-SD_lacZ, CMFDG, clindamycin, and an additional 15 μL of the CF-TXTL solutions based on the S150 cell extracts. The fluorescence of the reaction solutions was kinetically measured at 37 °C using Infinite® 200 PRO (TECAN) at λ_{ex} = 485 nm and λ_{em} = 535 nm.

Simultaneous synthesis of both SSU and LSU was conducted according to the protocol described above with minor modifications. In the first reaction, the concentrations of the native ribosomes, the artificial rRNA operon with or1-oASD, SpcR, and CldR, and 54 r-protein genes were 80, 0.9, and 0.01 nM each, respectively. In the second reaction, pT7_or1-oSD_LacZ and spectinomycin were used for the detection of the nascent artificial SSU, and pT7PCONS_EpsA20_WT-SD_lacZ and clindamycin were used for the detection of the nascent artificial LSU. pT7_or1-oSD_LacZ, spectinomycin, and clindamycin were used to detect the nascent artificial ribosomes. The reaction solution fluorescence was kinetically measured at 37 °C using Infinite® 200 PRO (TECAN) at λ_{ex} = 485 nm and λ_{em} = 535 nm.

Quantification of nascent artificial SSU and LSU was conducted as follows. For the quantification of nascent artificial SSU, a standard curve for the translational activity (ΔFluorescence (a.u.) min^{-1}) was generated under the same two-step experimental conditions used for the in vitro SSU biogenesis, except that spectinomycin and 80 nM native ribosomes were removed, and a specific amount of native ribosomes and the WT-SD–LacZ reporter were added in the second reaction. For the quantification of nascent artificial LSU, a standard curve for the translational activity (ΔFluorescence (a.u.) min^{-1}) was generated under the same two-step experimental conditions used for the in vitro LSU biogenesis, except that clindamycin and 80 nM native ribosomes were removed, and a specific amount of native ribosomes and the improved LacZ reporter were added in the second reaction. These standard curves represented the linear ranges of sigmoidal curves with the quantification limit defined as S/N > 5 and CV < 20%.

The iSAT assembly was performed according to previous reports[28,29,83] with some modifications. Briefly, in the first reaction, 15 μL of the CF-TXTL solutions based on the S150 cell extracts were mixed with 100 nM total protein of 70S ribosome (TP70) and 0.3 nM of the artificial rRNA operon with or1-oASD and SpcR. The solutions were incubated at 37 °C for 180 min. In the second reaction, the resulting CF-TXTL solutions were mixed with pT7_or1-oSD_LacZ, CMFDG, spectinomycin, and an additional 15 μL of the CF-TXTL solutions based on the S150 cell extracts. The reaction solution fluorescence was kinetically measured at 37 °C using Infinite® 200 PRO (TECAN) at λ_{ex} = 485 nm and λ_{em} = 535 nm. The standard curve of the translational activity of the iSAT reaction was generated under the same iSAT reaction condition, except that the artificial rRNA operon and spectinomycin were removed and that a specific amount of native ribosomes was added in the second reaction. The standard curve represented the linear range of a sigmoidal curve with the quantification limit defined as S/N > 5 and CV < 20%.

The parameter values described above were tuned experiment-dependently and are specified in the figure legends.

Femtoliter droplet assay

An oil mixture was composed of light mineral oil (Sigma-Aldrich Corporation, St. Louis, MO, USA), 4.5% sorbitan monooleate (Nacalai Tesque), and 0.5% Triton® X-100 (Nacalai Tesque)[84,85]. The CF-TXTL reaction solutions were mixed with the oil mixture and tapped twenty times in microtubes (Maruemu Corporations, Osaka, Japan). The emulsions were incubated at 37 °C. The bright-field and fluorescence images of droplets were obtained using a confocal fluorescence microscope LSM700 (Carl Zeiss AG, Oberkochen, Germany). The 488 nm laser was focused using an oil immersion objective (Plan-Apochromat 40×/1.4 Oil DIC M27, Carl Zeiss AG) with immersion oil (Immersol™ 518 F, Carl Zeiss AG).

Deep-learning-assisted automated femtoliter droplet assay

It is a difficult task to extract features from a large number of droplets; hence, we devised a deep-learning-assisted automated analysis pipeline for a scalable and objective droplet assay. We aimed to develop an analysis pipeline enabling area and centroid extraction of each droplet from the bright-field images and the fluorescence intensity of each droplet from the corresponding fluorescence images. In the beginning, we produced positive control fluorescent droplets using purified LacZ (FUJIFILM Wako Pure Chemical Corporation) and CMFDG and generated 15 sets of bright-field and corresponding fluorescence images containing 27580 fluorescent droplets in total. We trained an ilastik[86] pixel classification model and processed the positive control fluorescence images into binary segmented images (droplet or background) as ground truth. We used a convolutional neural network architecture called U-Net[48] to build a binary segmentation model. We used the FastAI library[87] under an Anaconda virtual environment (Python 3.7, torch = =1.4.0 + cpu, torchvision = =0.5.0 + cpu). The model was trained using 13 sets of ground-truth binary segmented images and the corresponding bright-field images, and the remaining two sets of images were used as test data. We specified an encoder network, Resnet34, and a weight-decay of 1e-2. We searched for a fitting learning rate using the learn.lr_find() method, and picked a learning rate of 1e-4. The model was trained using the fit_one_cycle() method for 20 epochs at slice(1e-4) and pct_start=0.3. We unfroze all layers and searched for a learning rate again. The whole model was trained using the fit_one_cycle() method for 100 epochs at slice(1e-4) and pct_start=0.3. As a result, the accuracy (number of correctly classified pixels/total number of pixels) reached > 90% using the test data (Supplementary Fig. 3). The trained U-Net deep-learning model was

used to process bright-field droplet images into binary segmented images, in which white and black regions indicate the droplets and background, respectively. The binary segmented images were provided for particle analysis using ImageJ, and the particle analysis results were redirected to corresponding fluorescence images. Using the deep-learning-assisted automated analysis pipeline, we could automatically obtain the area, mean fluorescence intensity, minimum fluorescence intensity, maximum fluorescence intensity, integrated density, and centroid of each droplet in a scalable and objective manner. The codes were described in Supplementary Data 4.

Sensitivity calculation of the droplet assay

We roughly estimated the sensitivity of the droplet assay using the data at 12 pM artificial ribosomes (dilution ratio 10^5) (Fig. 2B and Supplementary Fig. 5). In this experiment, a droplet with a diameter of 1 μm was expected to contain an average of 3.6×10^{-3} ribosomes, assuming that the artificial ribosomes in the cell extract did not form polysomes. This assumption is reasonable given that the artificial ribosomes do not interact with WT-SD–mRNA in cell extracts (Fig. 1F). From the Poisson distribution formula, the probability that a 1-μm droplet would contain k ribosomes was expressed as follows:

$$P(k,\lambda) = \frac{\lambda^k e^{-\lambda}}{k!} \quad (1)$$

where k is the number of ribosomes and λ is 3.6×10^{-3}. According to this formula, the ratios of droplets that contain zero, one, or two or more ribosomes were 0.996406, 0.003587, or 0.000007, respectively.

In the data at 12 pM artificial ribosomes (dilution ratio 10^5), we observed 15544 droplets with a diameter of 0.5–1.5 μm, and the number of fluorescent droplets among them was 17. The observed ratio of the fluorescent droplets was 0.0011. Taken together, most of the fluorescent droplets (99%) were estimated to contain only a single artificial ribosome.

Quantification of the artificial ribosome concentration in S12 cell extract

The ribosomes in the S12 cell extracts were purified as described previously[29] with some modifications. Specifically, BL21 Star™ (DE3) *lacZ::frt* expressing the artificial rRNA operon with or1-oASD and SpcR were grown in 1 L of 2 × YPTG medium at 37 °C. The cultured cells were harvested at OD_{600} of 3 and centrifuged. The cell pellets were resuspended in 4.5 mL buffer A for 1 g of wet cell paste and then disrupted using a Q125 Sonicator at a frequency input of 20 kHz and amplitude of 50%. The sonication energy input was 500 J for 1 mL cell suspension. The cell extract was centrifuged at 4 °C and 12,000 *g* for 10 min to collect the supernatant. The supernatant was centrifuged at 30,000 *g* for 30 min at 4 °C twice. The supernatant was collected and gently layered in ultracentrifuge tubes on top of a 3 mL sucrose cushion (20 mM HEPES, 10 mM $Mg(OAc)_2$, 30 mM NH_4Cl, 30 % sucrose, 7 mM 2-mercaptoethanol, pH = 7.2). The samples were then centrifuged at 150,000 *g* for 15 h at 4 °C. The clear ribosome pellet was washed and resuspended in a ribosome suspension buffer (20 mM HEPES, 30 mM K(OAc), 10 mM $Mg(OAc)_2$, 7 mM 2-mercaptoethanol, pH = 7.2), and its concentration was determined using the A_{260} NanoDrop readings (1 A_{260} unit of 70S = 24 pmol 70S)[29]. The concentration of ribosomes in the S12 cell extracts was 5.15 ± 0.51 μM (mean ± SD, n = 3). The resuspended ribosomes were then aliquoted and flash-frozen in liquid nitrogen and preserved at −80 °C until further use. rRNAs were sequenced by Bioengineering Lab. Co., Ltd. (Kanagawa, Japan). In brief, total RNA was purified using the RNeasy® Mini kit (QIAGEN) and sequenced using DNBSEQ-G400 (MGI Tech Co., Ltd., Shenzhen, China) at 2 × 100 bp. The concentration of the artificial ribosomes with or1-oASD and SpcR in the reaction solutions was estimated to be 1.2 ± 0.1 μM (mean ± SD, n = 3) by counting the number of reads derived from the artificial and native rRNAs.

Ribosome purification

Isolation of native SSU and LSU was performed through the protocol described below. *E. coli* ribosomes (New England BioLabs) were diluted 8-fold in 0% magnesium buffer (20 mM HEPES-KOH, 30 mM K(OAc), 7 mM 2-mercaptoethanol, pH = 7.6) and loaded onto a 10%–30% sucrose gradient solution (20 mM HEPES-KOH, 30 mM K(OAc), 0.5 mM $Mg(OAc)_2$, 7 mM 2-mercaptoethanol, pH = 7.6). After centrifugation at 150,000 *g* for 16 h at 4 °C using an Optima L-90K and SW 41 Ti swinging bucket rotor (Beckman Colter Inc., Brea, CA, USA), SSU and LSU were collected using a BioComp fractionator and concentrated using Amicon Ultra - 0.5 mL 100 kDa cutoff (Merck Millipore) and 70S buffer (20 mM HEPES-KOH, 150 mM K(OAc), 10 mM $Mg(OAc)_2$, 7 mM 2-mercaptoethanol, pH = 7.6). The concentration of the ribosomal subunits was determined based on its absorbance at 260 nm, as described previously[88]. Specifically, the concentration of ribosomes was determined using A_{260} measurements, where 1 A_{260} corresponds to 24 pmol ml^{-1} of 70S ribosomes, 36 pmol ml^{-1} of LSU, and 72 pmol ml^{-1} of SSU.

To purify the nascent artificial SSU and/or LSU, we constructed three plasmids encoding 16S rRNA with streptavidin-binding aptamer (Sb-aptamer)[89], 23S rRNA with Sb-aptamer, and both 16S and 23S rRNAs with Sb-aptamer, respectively. Sb-aptamer was inserted into the functionally neutral helix 33a of 16S rRNA and helix 25 of 23S rRNA as previously reported[59,60]. In vitro synthesis of SSU and LSU was performed as described above using the plasmids encoding the artificial rRNAs with Sb-aptamer. Nascent artificial SSU and/or LSU with Sb-aptamer were purified using streptavidin agarose under a subunit dissociation condition (1 mM Mg^{2+})[59]. Specifically, the reaction solutions were mixed with 50 μL streptavidin agarose (Thermo Fisher Scientific) and 1.5 mL ribosome dissociation buffer (20 mM HEPES-KOH, 1 mM magnesium glutamate, 200 mM potassium glutamate, and 4 mM DTT, pH = 7.5) and incubated for 16 h at 4 °C. The streptavidin agarose was washed seven times using 1 mL ribosome dissociation buffer to remove native subunits. The nascent artificial SSU and/or LSU with Sb-aptamer were eluted using ribosome dissociation buffer containing 25 mM biotin (Nacalai Tesque).

Mass spectrometric analysis

The proteomic analysis was carried out as previously described with modifications[90]. Specifically, the CF-TXTL reaction solutions were reduced by 50 mM DTT and modified with 50 mM iodoacetamide. For stable isotope labeling[91], we used CF-TXTL reaction solutions with 20 amino acid mixtures containing stable isotope-labeled (heavy) L-arginine ($^{13}C_6$, $^{15}N_4$) and L-lysine ($^{13}C_6$, $^{15}N_2$) (Thermo Fisher Scientific) instead of unlabeled (light) L-arginine and L-lysine. The proteins were digested with sequencing-grade modified trypsin (Promega Corporation). The peptides were analyzed using a nano LC–MS system (UltiMate™ 3000 RSLCnano and Orbitrap Exploris™ 240) equipped with an Aurora UHPLC column (AUR2-25075C18A; IonOpticks, Fitzroy, Australia). A gradient was produced by changing the mixing ratio of the two eluents: A, 0.1% (v/v) formic acid and B, acetonitrile. The gradient started with 5% B with a 10-min hold, was then increased to 45% B for 60 min, and finally increased to 95% B for a 10-min hold, following which the mobile phase was immediately adjusted to its initial composition and held for 10 min to re-equilibrate the column. The autosampler and column oven were maintained at 4 °C and 40 °C, respectively. The separated peptides were detected on the MS with a full-scan range of 300–2000 m/z (resolution of 240,000 or 60,000) in the positive mode followed by data-dependent MS/MS scans (resolution of 15,000) or parallel reaction monitoring. The data-dependent MS/MS analysis was set to automatically analyze the top 20 most intense ions observed in the MS scan. The ESI voltage, dynamic exclusion, ion-transfer tube temperature, and normalized collision

energy were 2 kV, 30 s, 275 °C, and 30%, respectively. The mass spectrometry data were analyzed using Proteome Discoverer 2.5 (Thermo Fisher Scientific). The protein identification was performed using Sequest HT against the protein database of *E. coli* DH5α (accession number PRJNA429943) with a precursor mass tolerance of 10 ppm, a fragment ion mass tolerance of 0.02 Da, and strict specificity allowing for up to 2 missed cleavage. Cysteine carbamidomethylation was set as a fixed modification. Methionine oxidation, N-terminus acetylation, and N-terminal methionine loss were set as dynamic modifications. Additionally, L-arginine ($^{13}C_6$, $^{15}N_4$) and L-lysine ($^{13}C_6$, $^{15}N_2$) were set as dynamic modifications for stable isotope labeling. The data were then filtered at a q-value ≤ 0.01 corresponding to a 1% false discovery rate on a spectral level. In parallel reaction monitoring, target peptides were automatically selected based on their *m/z* in MS1 followed by MS2 scans (resolution of 15,000). The selection was performed only around the retention time of each target peptide. The LC–MS/MS data was then analyzed using Skyline software[92] to annotate one or more fragment ions. The total number of samples analyzed is four. The number of biological replicates is two.

We analyzed the post-translational modifications of the nascent r-proteins by labeling them with heavy L-arginine ($^{13}C_6$, $^{15}N_4$) and L-lysine ($^{13}C_6$, $^{15}N_2$) (Thermo Fisher Scientific) in the CF-TXTL solution. The nascent r-proteins were then reduced with 50 mM DTT, modified with 50 mM iodoacetamide, and digested with sequencing-grade modified trypsin (Promega Corporation). The resultant peptides were analyzed by parallel reaction monitoring[93] using the same nano LC–MS system described above. The retention times of the peptides with post-translational modifications were determined by analyzing a tryptic digest of the *E. coli* ribosome (New England BioLabs). The total number of samples analyzed is two. The number of biological replicates is two.

The nascent artificial rRNA modifications were analyzed as follows. Nascent artificial ribosomes with Sb-aptamer were purified as described above. After extracting the rRNAs using the RNeasy® Mini kit (QIAGEN), their purity and size were determined using Bioanalyzer and the RNA 6000 pico Kit (Agilent, Santa Clara, CA, USA). RNA nucleoside mass spectrometry was performed as previously described[94]. Specifically, a 20 µL solution containing 9 ng of *E. coli*-derived or nascent artificial rRNAs, 20 mM HEPES-KOH (pH 7.6), 2 units of Nuclease P1 (FUJIFILM Wako Pure Chemical Corporation), and 0.25 units of bacterial alkaline phosphatase (Takara Bio, Shiga, Japan) was incubated at 37 °C for 3 h. The nucleoside solution (4 µL) was injected into the NEXERA X2–LCMS-8060 NX system (Shimadzu, Kyoto, Japan). The nucleosides were first separated on an Inertsil ODS-3 column (GL Sciences, Tokyo, Japan) using a mobile phase with a continuous gradient of 100% of solution A (5 mM ammonium acetate in water, pH 5.3) to 100% of solution B (60% acetonitrile in water) in 17 min at a flow rate of 0.4 mL min^{-1}, followed by electrospray ionization and triple quadrupole mass spectrometry in the multiple reaction monitoring mode. Temperatures for the interface, desolvation line, and heat block were 300 °C, 250 °C, and 400 °C, respectively. The *m/z* of the single-protonated precursor ion and product ion corresponding to each nucleoside species are as follows: G (284.0; 152.1), $m^6{}_2A$ (296.0; 164.0), m^1G (298.0; 166.0), Gm (298.1; 152.1), m^2A (282.3; 150.1), m^6A (282.3; 150.1), Cm (258.3; 112.1), m^5U (259.1; 127.0), m^5C (258.0;126.0), Ψ (245.1; 209.0), m^2G (298.0; 166.0), and m^7G (298.0; 166.0). The mass spectrometry data were analyzed using LabSolutions (Shimadzu). The total number of samples analyzed is seven. The number of biological replicates is two.

MS data are available in the jPOST repository[95] (JPST001809) and the MetaboLights repository[96] (MTBLS7425).

Reporting summary

Further information on research design is available in the Nature Portfolio Reporting Summary linked to this article.

Data availability

The data supporting the findings of this study are available from the corresponding authors upon request. NGS data generated in this study have been deposited in the NCBI Sequence Read Archive under accession code PRJNA974729. Mass spectrometry data generated in this study have been deposited in the jPOST and MetaboLights repositories under the accession code JPST001809 and MTBLS7425, respectively. The representative plasmid sequences are provided in Supplementary Data 5. Source data are provided with this paper.

Code availability

The code used in this study is provided in Supplementary Data 4 and Zenodo [https://zenodo.org/records/14209842][97].

References

1. De Capitani, J. & Mutschler, H. The long road to a synthetic self-replicating central dogma. *Biochemistry* **62**, 1221–1232 (2023).
2. Rothschild, L. J. et al. Building synthetic cells—from the technology infrastructure to cellular entities. *ACS Synth. Biol.* **13**, 974–997 (2024).
3. Kaczanowska, M. & Rydén-Aulin, M. Ribosome biogenesis and the translation process in *Escherichia coli*. *Microbiol. Mol. Biol. Rev.* **71**, 477–494 (2007).
4. Shajani, Z., Sykes, M. T. & Williamson, J. R. Assembly of bacterial ribosomes. *Annu. Rev. Biochem.* **80**, 501–526 (2011).
5. Talkington, M. W. T., Siuzdak, G. & Williamson, J. R. An assembly landscape for the 30S ribosomal subunit. *Nature* **438**, 628–632 (2005).
6. Adilakshmi, T., Bellur, D. L. & Woodson, S. A. Concurrent nucleation of 16S folding and induced fit in 30S ribosome assembly. *Nature* **455**, 1268–1272 (2008).
7. Mulder, A. M. et al. Visualizing ribosome biogenesis: parallel assembly pathways for the 30S subunit. *Science* **330**, 673–677 (2010).
8. Kim, H. et al. Protein-guided RNA dynamics during early ribosome assembly. *Nature* **506**, 334–338 (2014).
9. Davis, J. H. et al. Modular assembly of the bacterial large ribosomal subunit. *Cell* **167**, 1610–1622.e15 (2016).
10. Rodgers, M. L. & Woodson, S. A. Transcription increases the cooperativity of ribonucleoprotein assembly. *Cell* **179**, 1370–1381.e12 (2019).
11. Duss, O., Stepanyuk, G. A., Puglisi, J. D. & Williamson, J. R. Transient protein-RNA interactions guide nascent ribosomal RNA folding. *Cell* **179**, 1357–1369.e16 (2019).
12. Rabuck-Gibbons, J. N., Lyumkis, D. & Williamson, J. R. Quantitative mining of compositional heterogeneity in cryo-EM datasets of ribosome assembly intermediates. *Structure* **30**, 498–509.e4 (2022).
13. Nikolay, R. et al. Snapshots of native pre-50S ribosomes reveal a biogenesis factor network and evolutionary specialization. *Mol. Cell* **81**, 1200–1215.e9 (2021).
14. Li, N. et al. Cryo-EM structures of the late-stage assembly intermediates of the bacterial 50S ribosomal subunit. *Nucleic Acids Res* **41**, 7073–7083 (2013).
15. Champney, W. S. Kinetics of ribosome synthesis during a nutritional shift-up in *Escherischia coli* K-12. *Mol. Gen. Genet.* **152**, 259–266 (1977).
16. Kampen, K. R., Sulima, S. O., Vereecke, S. & De Keersmaecker, K. Hallmarks of ribosomopathies. *Nucleic Acids Res* **48**, 1013–1028 (2020).
17. Wang, K., Neumann, H., Peak-Chew, S. Y. & Chin, J. W. Evolved orthogonal ribosomes enhance the efficiency of synthetic genetic code expansion. *Nat. Biotechnol.* **25**, 770–777 (2007).
18. Orelle, C. et al. Protein synthesis by ribosomes with tethered subunits. *Nature* **524**, 119–124 (2015).

19. Schmied, W. H. et al. Controlling orthogonal ribosome subunit interactions enables evolution of new function. *Nature* **564**, 444–448 (2018).
20. Aleksashin, N. A. et al. Assembly and functionality of the ribosome with tethered subunits. *Nat. Commun.* **10**, 930 (2019).
21. Murase, Y., Nakanishi, H., Tsuji, G., Sunami, T. & Ichihashi, N. In vitro evolution of unmodified 16S rRNA for simple ribosome reconstitution. *ACS Synth. Biol.* **7**, 576–583 (2018).
22. Hammerling, M. J. et al. In vitro ribosome synthesis and evolution through ribosome display. *Nat. Commun.* **11**, 1108 (2020).
23. Mizushima, S. & Nomura, M. Assembly mapping of 30S ribosomal proteins from *E. coli*. *Nature* **226**, 1214 (1970).
24. Röhl, R. & Nierhaus, K. H. Assembly map of the large subunit (50S) of *Escherichia coli* ribosomes. *Proc. Natl Acad. Sci. USA* **79**, 729–733 (1982).
25. Culver, G. M. & Noller, H. F. Efficient reconstitution of functional *Escherichia coli* 30S ribosomal subunits from a complete set of recombinant small subunit ribosomal proteins. *RNA* **5**, 832–843 (1999).
26. Nierhaus, K. H. & Dohme, F. Total reconstitution of functionally active 50S ribosomal subunits from *Escherichia coli*. *Proc. Natl Acad. Sci. USA* **71**, 4713–4717 (1974).
27. Traub, P. & Nomura, M. Structure and function of *E. coli* ribosomes. V. reconstitution of functionally active 30S ribosomal particles from RNA and proteins. *Proc. Natl Acad. Sci. USA* **59**, 777–784 (1968).
28. Jewett, M. C., Fritz, B. R., Timmerman, L. E. & Church, G. M. In vitro integration of ribosomal RNA synthesis, ribosome assembly, and translation. *Mol. Syst. Biol.* **9**, 678 (2013).
29. Fritz, B. R. & Jewett, M. C. The impact of transcriptional tuning on in vitro integrated rRNA transcription and ribosome construction. *Nucleic Acids Res* **42**, 6774–6785 (2014).
30. Shimojo, M. et al. In vitro reconstitution of functional small ribosomal subunit assembly for comprehensive analysis of ribosomal elements in *E. coli*. *Commun. Biol.* **3**, 142 (2020).
31. Aoyama, R. et al. In vitro reconstitution of the *Escherichia coli* 70S ribosome with a full set of recombinant ribosomal proteins. *J. Biochem.* **171**, 227–237 (2022).
32. Nikolay, R. et al. Structural visualization of the formation and activation of the 50s ribosomal subunit during in vitro reconstitution. *Mol. Cell* **70**, 881–893.e3 (2018).
33. Qin, B. et al. Cryo-EM captures early ribosome assembly in action. *Nat. Commun.* **14**, 898 (2023).
34. Dong, X. et al. Near-physiological in vitro assembly of 50S ribosomes involves parallel pathways. *Nucleic Acids Res* **51**, 2862–2876 (2023).
35. Dong, X. et al. Assembly of the bacterial ribosome with circularly permuted rRNA. *Nucleic Acids Res*. https://doi.org/10.1093/nar/gkae636 (2024).
36. Li, J. et al. Cogenerating synthetic parts toward a self-replicating system. *ACS Synth. Biol.* **6**, 1327–1336 (2017).
37. Levy, M., Falkovich, R., Daube, S. S. & Bar-Ziv, R. H. Autonomous synthesis and assembly of a ribosomal subunit on a chip. *Sci. Adv.* **6**, eaaz6020 (2020).
38. Jewett, M. C. & Swartz, J. R. Mimicking the *Escherichia coli* cytoplasmic environment activates long-lived and efficient cell-free protein synthesis. *Biotechnol. Bioeng.* **86**, 19–26 (2004).
39. Igarashi, K. & Kashiwagi, K. Effects of polyamines on protein synthesis and growth of *Escherichia coli*. *J. Biol. Chem.* **293**, 18702–18709 (2018).
40. Hui, A. & de Boer, H. A. Specialized ribosome system: preferential translation of a single mRNA species by a subpopulation of mutated ribosomes in *Escherichia coli*. *Proc. Natl Acad. Sci. USA* **84**, 4762–4766 (1987).
41. Rackham, O. & Chin, J. W. A network of orthogonal ribosome x mRNA pairs. *Nat. Chem. Biol.* **1**, 159–166 (2005).
42. Chubiz, L. M. & Rao, C. V. Computational design of orthogonal ribosomes. *Nucleic Acids Res* **36**, 4038–4046 (2008).
43. Carlson, E. D. et al. Engineered ribosomes with tethered subunits for expanding biological function. *Nat. Commun.* **10**, 3920 (2019).
44. Rondelez, Y. et al. Microfabricated arrays of femtoliter chambers allow single molecule enzymology. *Nat. Biotechnol.* **23**, 361–365 (2005).
45. Szostak, J. W., Bartel, D. P. & Luisi, P. L. Synthesizing life. *Nature* **409**, 387–390 (2001).
46. Shine, J. & Dalgarno, L. The 3′-terminal sequence of *Escherichia coli* 16S ribosomal RNA: complementarity to nonsense triplets and ribosome binding sites. *Proc. Natl Acad. Sci. USA* **71**, 1342–1346 (1974).
47. Sigmund, C. D., Ettayebi, M. & Morgan, E. A. Antibiotic resistance mutations in 16S and 23S ribosomal RNA genes of *Escherichia coli*. *Nucleic Acids Res* **12**, 4653–4663 (1984).
48. Ronneberger, O., Fischer, P. & Brox, T. U-Net: Convolutional Networks for Biomedical Image Segmentation. in *Medical Image Computing and Computer-Assisted Intervention – MICCAI 2015* 234–241 (Springer International Publishing, 2015).
49. Schneider, C. A., Rasband, W. S. & Eliceiri, K. W. NIH Image to ImageJ: 25 years of image analysis. *Nat. Methods* **9**, 671–675 (2012).
50. Fiordemondo, D. & Stano, P. Lecithin-based water-in-oil compartments as dividing bioreactors. *Chembiochem* **8**, 1965–1973 (2007).
51. Kato, A., Yanagisawa, M., Sato, Y. T., Fujiwara, K. & Yoshikawa, K. Cell-sized confinement in microspheres accelerates the reaction of gene expression. *Sci. Rep.* **2**, 283 (2012).
52. Marshall, R. & Noireaux, V. Quantitative modeling of transcription and translation of an all-*E. coli* cell-free system. *Sci. Rep.* **9**, 11980 (2019).
53. Caschera, F. et al. High-throughput optimization cycle of a cell-free ribosome assembly and protein synthesis system. *ACS Synth. Biol.* **7**, 2841–2853 (2018).
54. Doerr, A. et al. Modelling cell-free RNA and protein synthesis with minimal systems. *Phys. Biol.* **16**, 025001 (2019).
55. Cochella, L. & Green, R. Isolation of antibiotic resistance mutations in the rRNA by using an in vitro selection system. *Proc. Natl Acad. Sci. USA* **101**, 3786–3791 (2004).
56. Shilling, P. J. et al. Improved designs for pET expression plasmids increase protein production yield in *Escherichia coli*. *Commun. Biol.* **3**, 214 (2020).
57. Takahashi, S., Furusawa, H., Ueda, T. & Okahata, Y. Translation enhancer improves the ribosome liberation from translation initiation. *J. Am. Chem. Soc.* **135**, 13096–13106 (2013).
58. Chumpolkulwong, N. et al. Effects of *Escherichia coli* ribosomal protein S12 mutations on cell-free protein synthesis. *Eur. J. Biochem.* **271**, 1127–1134 (2004).
59. Leonov, A. A., Sergiev, P. V., Bogdanov, A. A., Brimacombe, R. & Dontsova, O. A. Affinity purification of ribosomes with a lethal G2655C mutation in 23 S rRNA that affects the translocation. *J. Biol. Chem.* **278**, 25664–25670 (2003).
60. Golovina, A. Y., Bogdanov, A. A., Dontsova, O. A. & Sergiev, P. V. Purification of 30S ribosomal subunit by streptavidin affinity chromatography. *Biochimie* **92**, 914–917 (2010).
61. Sergiev, P. V., Aleksashin, N. A., Chugunova, A. A., Polikanov, Y. S. & Dontsova, O. A. Structural and evolutionary insights into ribosomal RNA methylation. *Nat. Chem. Biol.* **14**, 226–235 (2018).
62. Kimura, S. & Suzuki, T. Iron-sulfur proteins responsible for RNA modifications. *Biochim. Biophys. Acta* **1853**, 1272–1283 (2015).
63. Chen, S. S., Sperling, E., Silverman, J. M., Davis, J. H. & Williamson, J. R. Measuring the dynamics of E. coli ribosome biogenesis using pulse-labeling and quantitative mass spectrometry. *Mol. Biosyst.* **8**, 3325–3334 (2012).
64. Pulk, A. et al. Ribosome reactivation by replacement of damaged proteins. *Mol. Microbiol.* **75**, 801–814 (2010).

65. Subramanian, A. R. & van Duin, J. Exchange of individual ribosomal proteins between ribosomes as studied by heavy isotope-transfer experiments. *Mol. Gen. Genet.* **158**, 1–9 (1977).
66. Robertson, W. R., Dowsett, S. J. & Hardy, S. J. Exchange of ribosomal proteins among the ribosomes of *Escherichia coli*. *Mol. Gen. Genet.* **157**, 205–214 (1977).
67. Kolber, N. S., Fattal, R., Bratulic, S., Carver, G. D. & Badran, A. H. Orthogonal translation enables heterologous ribosome engineering in *E. coli*. *Nat. Commun.* **12**, 599 (2021).
68. Kaguni, J. M. & Kornberg, A. Replication initiated at the origin (*oriC*) of the *E. coli* chromosome reconstituted with purified enzymes. *Cell* **38**, 183–190 (1984).
69. Su'etsugu, M., Takada, H., Katayama, T. & Tsujimoto, H. Exponential propagation of large circular DNA by reconstitution of a chromosome-replication cycle. *Nucleic Acids Res* **45**, 11525–11534 (2017).
70. Chamberlin, M. & Berg, P. Deoxyribo ucleic acid-directed synthesis of ribonucleic acid by an enzyme from *Escherichia coli*. *Proc. Natl Acad. Sci. USA* **48**, 81–94 (1962).
71. Nirenberg, M. W. & Matthaei, J. H. The dependence of cell-free protein synthesis in *E. coli* upon naturally occurring or synthetic polyribonucleotides. *Proc. Natl Acad. Sci. USA* **47**, 1588–1602 (1961).
72. Shimizu, Y. et al. Cell-free translation reconstituted with purified components. *Nat. Biotechnol.* **19**, 751–755 (2001).
73. Yue, K., Chen, J., Li, Y. & Kai, L. Advancing synthetic biology through cell-free protein synthesis. *Comput. Struct. Biotechnol. J.* **21**, 2899–2908 (2023).
74. Datsenko, K. A. & Wanner, B. L. One-step inactivation of chromosomal genes in *Escherichia coli* K–12 using PCR products. *Proc. Natl Acad. Sci. USA* **97**, 6640–6645 (2000).
75. Huang, S. et al. Ribosome engineering reveals the importance of 5S rRNA autonomy for ribosome assembly. *Nat. Commun.* **11**, 2900 (2020).
76. Lewicki, B. T., Margus, T., Remme, J. & Nierhaus, K. H. Coupling of rRNA transcription and ribosomal assembly in vivo. formation of active ribosomal subunits in *Escherichia coli* requires transcription of rRNA genes by host RNA polymerase which cannot be replaced by bacteriophage T7 RNA polymerase. *J. Mol. Biol.* **231**, 581–593 (1993).
77. Iskakova, M. B., Szaflarski, W., Dreyfus, M., Remme, J. & Nierhaus, K. H. Troubleshooting coupled in vitro transcription-translation system derived from *Escherichia coli* cells: synthesis of high-yield fully active proteins. *Nucleic Acids Res* **34**, e135 (2006).
78. Boni, I. V., Isaeva, D. M., Musychenko, M. L. & Tzareva, N. V. Ribosome-messenger recognition: mRNA target sites for ribosomal protein S1. *Nucleic Acids Res* **19**, 155–162 (1991).
79. Komarova, A. V., Tchufistova, L. S., Supina, E. V. & Boni, I. V. Protein S1 counteracts the inhibitory effect of the extended Shine-Dalgarno sequence on translation. *RNA* **8**, 1137–1147 (2002).
80. Chen, S. S. & Williamson, J. R. Characterization of the ribosome biogenesis landscape in *E. coli* using quantitative mass spectrometry. *J. Mol. Biol.* **425**, 767–779 (2013).
81. Sheahan, T. & Wieden, H.-J. Ribosomal protein S1 improves the protein yield of an in vitro reconstituted cell-free translation system. *ACS Synth. Biol.* **11**, 1004–1008 (2022).
82. Kwon, Y.-C. & Jewett, M. C. High-throughput preparation methods of crude extract for robust cell-free protein synthesis. *Sci. Rep.* **5**, 8663 (2015).
83. Fritz, B. R., Jamil, O. K. & Jewett, M. C. Implications of macromolecular crowding and reducing conditions for in vitro ribosome construction. *Nucleic Acids Res* **43**, 4774–4784 (2015).
84. Griffiths, A. D. & Tawfik, D. S. Directed evolution of an extremely fast phosphotriesterase by in vitro compartmentalization. *EMBO J.* **22**, 24–35 (2003).
85. Murzabaev, M. et al. Handmade microfluidic device for biochemical applications in emulsion. *J. Biosci. Bioeng.* **121**, 471–476 (2016).
86. Berg, S. et al. ilastik: interactive machine learning for (bio)image analysis. *Nat. Methods* **16**, 1226–1232 (2019).
87. Howard, J. & Gugger, S. Fastai: a layered API for deep learning. *Information* **11**, 108 (2020).
88. Christodoulou, J. et al. Heteronuclear NMR investigations of dynamic regions of intact *Escherichia coli* ribosomes. *Proc. Natl Acad. Sci. USA* **101**, 10949–10954 (2004).
89. Bachler, M., Schroeder, R. & von Ahsen, U. StreptoTag: a novel method for the isolation of RNA-binding proteins. *RNA* **5**, 1509–1516 (1999).
90. Tsuji, T. et al. YAP1 mediates survival of ALK-rearranged lung cancer cells treated with alectinib via pro-apoptotic protein regulation. *Nat. Commun.* **11**, 74 (2020).
91. Ong, S.-E. et al. Stable isotope labeling by amino acids in cell culture, SILAC, as a simple and accurate approach to expression proteomics. *Mol. Cell. Proteom.* **1**, 376–386 (2002).
92. MacLean, B. et al. Skyline: an open source document editor for creating and analyzing targeted proteomics experiments. *Bioinformatics* **26**, 966–968 (2010).
93. Peterson, A. C., Russell, J. D., Bailey, D. J., Westphall, M. S. & Coon, J. J. Parallel reaction monitoring for high resolution and high mass accuracy quantitative, targeted proteomics. *Mol. Cell. Proteom.* **11**, 1475–1488 (2012).
94. Nagayoshi, Y. et al. Loss of Ftsj1 perturbs codon-specific translation efficiency in the brain and is associated with X-linked intellectual disability. *Sci. Adv.* **7**, eabf3072 (2021).
95. Okuda, S. et al. jPOSTrepo: an international standard data repository for proteomes. *Nucleic Acids Res* **45**, D1107–D1111 (2017).
96. Haug, K. et al. MetaboLights: a resource evolving in response to the needs of its scientific community. *Nucleic Acids Res* **48**, D440–D444 (2020).
97. Aoki, W. Ribosome biogenesis in vitro. https://doi.org/10.5281/ZENODO.14209841 (2022).

Acknowledgements

The authors would like to thank Kei Fujiwara for useful discussions. This work was supported by JSPS KAKENHI (grant numbers 19K16109, 26830139, 23K18110, and 23K26466 to WA), JSPS Research Fellowship for Young Scientists (grant number 22J22251 to YK), JST FOREST (grant number JPMJFR204K to WA), Joint Research of the Exploratory Research Center on Life and Living Systems (ExCELLS, program No. 22EXC601 to WA), JST START University Ecosystem Promotion Type (Supporting Creation of Startup Ecosystem in Startup Cities, grant number JPMJST2181 to WA), JST GteX (grant number JPMJGX23B4 to WA), Sugiyama Chemical & Industrial Laboratory (http://www.sugiyama-c-i-l.or.jp/ to WA), JGC-S Scholarship Foundation (https://www.jgcs.or.jp/en/ to WA). The funders did not have any role in the study design, data collection and analysis, decision to publish, or preparation of the manuscript.

Author contributions

Conceptualization: W.A., Research design: Y.K., Y.M., W.A., Investigation: Y.K., Y.M., W.A., Mass spectrometric analysis: S.A., C.N., T.C., K.T., W.A., Preparation of cell extracts: Y.K., Y.M., M.M., Droplet assay: Y.K., Y.M., M.F., W.A., Ribosome purification, Y.K., T.N., T.M., T.S., H.T., W.A., Supervision: K.S., M.U., W.A., Writing—original draft: Y.K., Y.M., W.A., Writing—review & editing: all authors.

Competing interests

Kyoto University have filed a patent application on in vitro ribosome biogenesis (by YK and WA). TS is employed at TechnoPro, Inc. These competing interests do not alter our adherence to the journal policies on sharing data and materials. The other authors declare no competing interests.

Additional information

Supplementary information The online version contains supplementary material available at https://doi.org/10.1038/s41467-025-55853-7.

Correspondence and requests for materials should be addressed to Wataru Aoki.

Peer review information *Nature Communications* thanks Takuhiro Ito, who co-reviewed with Alexander Wagner and the other, anonymous, reviewer(s) for their contribution to the peer review of this work. A peer review file is available.